ACS APPLIED MATERIALS & INTERFACES

Research Article

www.acsami.org

Structural Coloration of Colloidal Fiber by Photonic Band Gap and Resonant Mie Scattering

Wei Yuan,[†] Ning Zhou,[†] Lei Shi,[‡,§] and Ke-Qin Zhang*[,†]

[†]National Engineering Laboratory for Modern Silk, College for Textile and Clothing Engineering, Soochow University, Suzhou, Jiangsu 215123, PR China

[‡]Department of Physics, Key Laboratory of Micro & Nano Photonic Structures (MOE) and Key Laboratory of Surface Physics, Fudan University, Shanghai 200433, PR China

[§]Collaborative Innovation Center of Advanced Microstructures, Nanjing University, Nanjing 210093, PR China

Supporting Information

ABSTRACT: Because structural color is fadeless and dye-free, structurally colored materials have attracted great attention in a wide variety of research fields. In this work, we report the use of a novel structural coloration strategy applied to the fabrication of colorful colloidal fibers. The nanostructured fibers with tunable structural colors were massively produced by colloidal electrospinning. Experimental results and theoretical modeling reveal that the homogeneous and noniridescent structural colors of the electrospun fibers are caused by two phenomena: reflection due to the band gap of photonic structure and Mie scattering of the colloidal spheres. Our unprecedented findings show promise in paving way for the development of revolutionary dye-free technology for the coloration of various fibers.

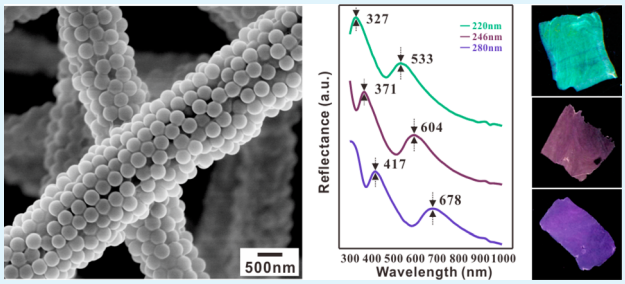

KEYWORDS: *structural coloration, colloidal electrospinning, photonic band gap, Mie scattering, noniridescent*

INTRODUCTION

Dyeing is an ancient technique for coloring the fabrics by fixing the natural or synthetic dyes, which absorb and reflect light at specific wavelengths to give human eyes the sense of color.[1] However, the dyeing process causes severe water pollution due to contamination from residual colorants, which is impossible to naturally degrade.[2] Although many new dyeing technologies have been introduced in an attempt to reduce the pollution, it is inevitable that chemical dyes and synthetic pigments will be used in the coloration process for textile products.[3,4] To transcend this obstacle, a revolutionary coloration strategy is required to replace the dyeing process.

Countless colors can be found in nature, and some are caused by diverse interactions between light and complicated nanostructures. These colors, called structural colors,[5−8] are formed without the incorporation of dyes. The physical mechanisms of structural colors have been subject to intensive investigation by researchers.[9−15] One explanation for structural coloration ascribes this phenomenon to the photonic band gap of ordered photonic structures, which mostly appear in the feathers of birds and skins of beetles.[9,10] The incident light is coherently scattered by periodic photonic crystals (PCs). This scattering results in strong reflection of specific frequencies of light, which determine the object's color. Additionally, because of the anisotropic structure of PCs, the observed color depends on the angle of incident light; this phenomenon is known as iridescence.[11,12]

Mie scattering is another mechanism used to explain coloration in some natural phenomenon.[16−25] Incident light scattered by a single scatter results in portions of light within certain frequencies being strongly scattered. The frequency of the scattered light always corresponds to certain electromagnetic multipolar modes supported by the scattering. When the scattering is randomly distributed in space, incoherent multiple scattering appears, significantly differing from periodic structure. In such cases, the light is strongly scattered within a resonant frequency range determined by the properties of a single scatter. Therefore, the randomly arranged scattering results in noniridescent color.[17−25]

Because of increased awareness of ecological sustainability, development of dye-free fibers based on natural coloration is a growing area of research.[26−33] Several groups have recently attempted fabricating structurally colored cylindrical fibers,[26−30,33,34] with a general concept of using colloidal spheres to form a periodic structure along the fibers. Colors observed in the resulting fibers are due to coherent scattering caused by the periodicity in the radial direction, giving constructively reflected light in a certain frequency. Because of the axial symmetry of structures with cylindrical geometry, the color of the periodic structured fiber is noniridescent when the direction of the

Received: April 16, 2015
Accepted: June 11, 2015
Published: June 11, 2015

DOI: 10.1021/acsami.5b03289
ACS Appl. Mater. Interfaces 2015, 7, 14064−14071

incident light is perpendicular to the fiber axis. However, iridescence still appears if the axial direction component of the incident light is nonzero. Although several ways to fabricate of structural-colored fibers was reported,[26−33] there are currently no practical fabrication methods that are compatible with industrial textile applications. Three concerns must be addressed when considering industrial applications: mass-production, linear density of yarn, and homogeneous nondirectional observation of color. The liner density of yarn is notable, as this property determines fabric warmth and comfort, and directly correlates to the fiber diameter. Fabrication of structural color fiber with the diameter of only several micrometers has not yet been achieved, and its realization is key to its applicability for uses in the textile industry. Because of usage habits developed over thousands of years, people are already familiar with homogeneous and nondirectional observation of the color in their clothing and other textile-based possessions. Although normal artificial structural colors possess unique special properties with beneficial applications, their unfamiliar iridescent effect and inhomogeneous scattering create reluctance for widespread usage of structural colors in the textile industry.

In this work, we massively produced uniform colloidal fibers via colloidal electrospinning method. After being treated with water, the dye-free eletrospun fibrous membrane (FM) with tunable structural colors was successfully prepared. And the special optical properties of the prepared colorful membranes were studied by both experiment and computer simulation. The homogeneous and noniridescent coloration method may provide a step toward the development of dye-free coloration strategies for textiles and other practical coloration processes.

EXPERIMENTAL SECTION

Materials. All chemicals are reagent grade and were used without further purification as purchased. Styrene (St), methyl methacrylate (MMA), acrylic acid (AA), ammonium persulfate (APS), sodium dodecyl benzenesulfonate (SDBS), ammonium bicarbonate, ethanol, concentrated sulfuric acid (98%), and diluted hydrofluoric (HF) acid were purchased from Shanghai Chemical Reagent Co. Ltd. (China). Poly(vinyl alcohol) (PVA, M_w =145 000, 99% hydrolyzed) was purchased from Sigma-Aldrich. Deionized (DI) water was used in all the experiments. Fused silica (10 μm in diameter) capillary tubes (SCT) were purchased from Polymicro Technologies.

Synthesis of Monodispersed P(St-MMA-AA) Composite Nanospheres. Monodispersed composite latex spheres of poly(styrene-methyl methacrylate-acrylic acid) (P(St-MMA-AA)) were synthesized by emulsion polymerization following reported procedures.[35] Briefly, St (20 g), MMA (1 g), AA (1 g), DI water (100 g), SDBS (0−0.004 g), and ammonium bicarbonate (0.5 g) were added sequentially into a four-necked flask equipped with an N_2 inlet, a reflux condenser and a mechanical stirrer at stirring speed of 300 rpm. The reaction mixture was initially performed at 70 °C for 30 min. Following the addition of a aqueous solution APS (0.48 g dissolved in 15 g DI water), polymerization was carried out at 80 °C for 10 h with continuous stirring. The resulting latex spheres were washed three times by centrifugation and redispersed in DI water by ultrasonication.

Preparation of Colloidal Fiber and Colorful FM. As shown in Figure 1, the electrospun precursor solution was prepared by blending 1 mL P(St-MMA-AA) colloidal dispersion with high concentration of 40 wt % and a measured amount of poly(vinyl alcohol) (PVA) solution with 13 wt % concentrations. The weight ratio of PVA to P(St-MMA-AA) colloidal spheres was 1:4, in which the latex spheres dominated in the blend solution.[36] The mixture was stirred vigorously for at least 3 h at room temperature and ultrasonically treated for 5 min to obtain a homogeneous milky solution. The resulting viscous solution was transferred into a 5 mL plastic syringe connected with a metallic needle of 0.5 mm inner diameter. The syringe was fixed vertically and the solution was fed at a constant and controllable rate of 0.5 mL/h by using a microinjection pump (LSP02−1B, Baoding Longer Precision Pump Co., Ltd., China). Using a power supply (DW-P303−1AC, Tianjin Dongwen High Voltage Co., China), a high voltage of 10 kV was applied between the needle and collector, generating a continuous jetting stream. The white electrospun membranes were collected on the surface of a grounded copper plate covered by aluminum foil, with collecting distance of 15 cm. Finally, the obtained electrospun FMs were fixed on the black PE plates (2 cm × 2 cm) and immersed into 100 mL DI water for 2 h at room temperature. The treated membranes dried under vacuum for 4 h, resulting in the structurally colored FMs.

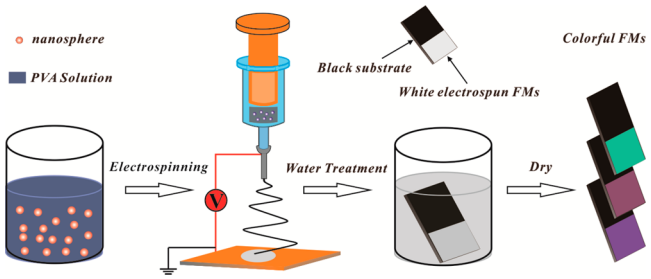

Figure 1. Schematic illustration of the process of colloidal electrospinning and fabrication of colorful FMs.

Characterization. The morphologies of colloidal spheres, colloidal crystal fibers, colloidal crystal film, electrospun membranes before and after water treatment were observed by a field emission scanning electron microscope (FE-SEM) (S-4800, Hitachi Ltd., Japan). The samples were sputtered with gold film before SEM observation. The mean size and polydispersity of colloidal spheres were measured by dynamic light scattering (Zetasizer Nano S90, Malvern Instruments Ltd., England). The diameters of electrospun fibers were measured from SEM images using image analysis software (ImageJ 1.44p, National Institutes of Health, USA). At least 100 measurements were analyzed per sample and the resulting measurements were made from multiple images. Fourier transform infrared (FTIR) spectra were recorded in the range 200−4000 cm^{-1}(Thermo Nicolet 5700, Thermo Fisher Scientific Inc., USA). Thermal property analysis of the colloidal electrospun FM was studied using a thermogravimetric analyzer (Diamond TG/DTA, PerkinElmer), at temperatures ranging from 30 to 600 °C, increasing at a rate of 5 °C/min. Pictures of colorful electrospun FMs were taken by Nikon DSLR camera (D5100) under ordinary white light. Optical images of colloidal crystal fibers were taken by dark-field optical microscope (BX51W1, Olympus, Japan). All reflective and scattering spectra were collected from angle-resolved microspectroscopy system (ARM160, Ideaoptics, PR China).

RESULTS AND DISCUSSION

The P(St-MMA-AA) composite colloidal sphere was chosen as the solid content of the electrospinning dope. Figure 2a shows

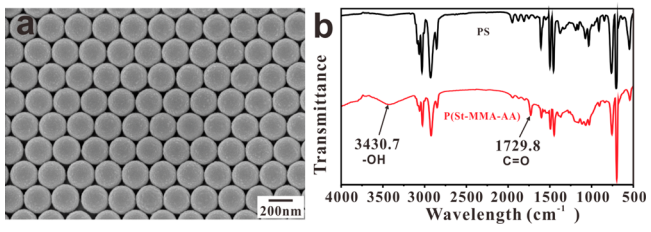

Figure 2. (a) Typical SEM image of P(St-MMA-AA) composite colloidal sphere. (b) FTIR spectra of pure PS and P(St-MMA-AA) colloidal spheres. The diameter of the composite colloidal sphere is 220 nm.

DOI: 10.1021/acsami.5b03289
ACS Appl. Mater. Interfaces 2015, 7, 14064−14071

the SEM image of obtained latex spheres with diameter of 220 nm. It can been seen clearly that the composite colloidal spheres with spherical shape and smooth surface were exceptionally uniform in size distribution. According to previous research,[35] large amounts of carboxyl groups were grafted on the surface of P(St-MMA-AA) composite colloidal spheres. To verify the above results, the pure PS and P(St-MMA-AA) composite colloidal sphere were analyzed by FTIR spectra as shown in Figure 2b. In addition to the typical absorption bands of PS, the composite colloidal sphere has the characteristic bands of hydroxyl (−OH) and carbonyl (C═O) at 3430.7 and 1729.8 cm^{-1}, which certified the existence of carboxyl groups on the surface of P(St-MMA-AA) colloidal sphere. Massive carboxyl groups anchored upon the surface of latex spheres, contributing to the formation of hydrogen bonds between colloidal spheres and PVA during the subsequent mixing and electrospinning process.

Subsequently, colloidal fibers are massively produced by colloidal electrospinning method.[36,37] Colloidal electrospinning is related with but significantly varies from conventional electrospinning,[38,39] as it incorporates the colloidal nanoparticles into the polymer solution. Figure 1 shows the setup used to fabricate the colloidal fibers. The uniform colloidal fibers were electrospun from a blend solution of P(St-MMA-AA) composite colloidal spheres and PVA solution; PVA served to adhere the spheres, forming colloidal fibers. In our previous research,[36] it has been indicated that a thin layer PVA was wrapped on P(St-MMA-AA) spheres during the mixing process. The soft shell acts as binder to provide the adhesive force between colloidal spheres. During the electrospinning, the wrapped colloidal spheres were packed and thinned into the fibers. To quantify the mass ratio of PVA and P(St-MMA-AA) composite spheres to form colloidal fibers, we performed thermogravimetric analysis (TGA) on the obtained electrospun FM as shown in Figure S1 in the Supporting Information. The decreases in mass at 17.2643 and 80.8231% were attributed to the decomposition of PVA and P(St-MMA-AA) at different temperature stages, which indicated the weight ratio (PVA/P(St-MMA-AA)) was about 1:4.6 in the electropun colloidal FM. The massively produced colloidal fibers were deposited on the collector to form the nonwowen FM during the electrospinning process. Figure 3a shows the picture of prepared electrospun FM composed of colloidal fibers with 220 nm colloidal sphere. The SEM image of electrospun FM (Figure 3a) with low magnification as shown in Figure 3b indicates that the colloidal fibers were extremely uniform in size distribution. Despite being packed with 220 nm colloidal spheres, the diameter of the obtained colloidal fiber was only 1.35 ± 0.3 μm, as shown in Figures S2 in the Supporting Information. Figure 3c−e shows the SEM images of colloidal fibers with 220, 246, and 280 nm colloidal spheres, respectively. It was clearly that the colloidal spheres were cylindrically packed with a local hexagonal order, as shown the areas marked with red dotted line in Figure 3c−e. The massively produced colloidal fibers were as soft as commercial textile fibers such as cotton and polyester. Single strand of the colloidal fiber can even be folded in half, as shown in Figure 3f; these fibers are more flexible than colloidal crystal structures self-assembled in certain patterns.[26] However, the prepared FMs were white (Figure 3a) without any structural color, and their spectral reflectance reached 70% in the range of visible wavelength, as shown in Figure S3 in the Supporting Information. We speculate that the resulting FMs were colorless because of the low refractive index contrast and P(St-MMA-AA)'s low intrinsic absorption in the visible region.

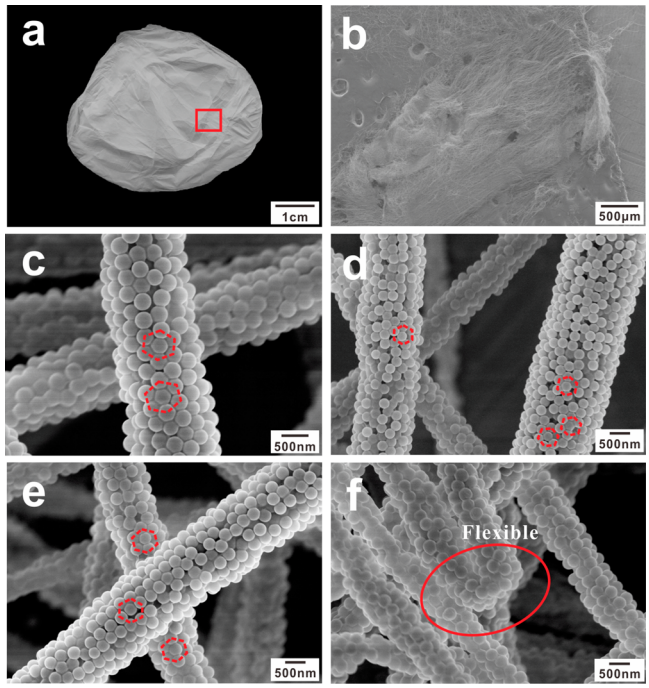

Figure 3. (a) Optical image of the electrospun FM of colloidal fibers (with 220 nm colloidal sphere). (b) SEM image of the area marked with red solid line in (a) with low magnification. (c−e) Clear morphologies of colloidal fibers composed of 220, 246, and 280 nm, respectively. The local hexagonal order along fibers was marked with red dotted line. (f) SEM image of the colloidal fiber with fold structure, and the folded area along the fiber was marked with red solid line (with 220 nm colloidal sphere).

To verify our conjecture, we immersed the electrospun FMs in deionized water for 2 h and dried at room temperature. Interestingly, the membrane appeared colored after water treatment. In this process, a large amount of PVA was dissolved in water and removed from the structure, increasing the refractive index contrast.[40] Although being treated with water, the FM preserved its fibrous shape, as shown in SEM images with different magnification of Figure 4a−c. The treated colloidal fibers were piled up randomly to form the colorful FMs. Some of the undissolved PVA connected the colloidal spheres with structure of nanofibers as shown in the area marked with red dotted line of Figure 4c. Green, red, and purplish-red FMs were prepared using colloidal spheres measuring 220, 246, and 280 nm, respectively. The optical images and corresponding reflective spectra of the FMs are shown in Figure 4d−f and Figure S4 in the Supporting Information. The typical reflective spectra of the colorful FMs possessed two characteristic peaks that contribute to their structural colors. The FMs composed of 220 and 246 nm spheres had peaks located in the ultraviolet range, at 327 and 371 nm, respectively. These FMs also had peaks at 533 and 604 nm, just within the visible range, resulting in green and red colors. The FM prepared using 280 nm spheres had two longer reflective peaks at 417 and 678 nm, exhibiting color mixing due to the dual visible reflections. Furthermore, the bendability of the colorful FM was studied as shown in Figure S5 in the Supporting Information. The colorful FM was tightly attached on the PE substrate after water treatment, Figure S5a in the

DOI: 10.1021/acsami.5b03289
ACS Appl. Mater. Interfaces 2015, 7, 14064−14071

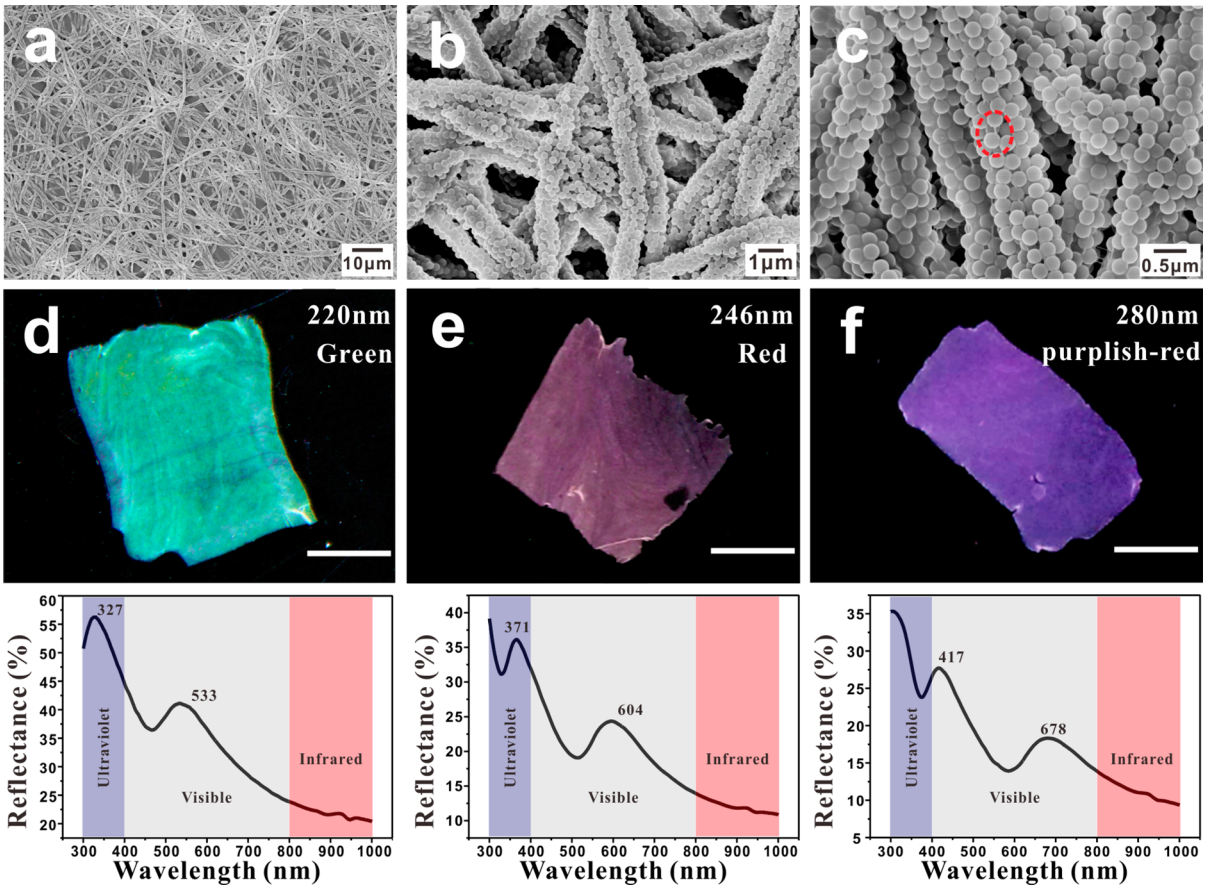

Figure 4. Typical SEM images of electrospun FM (with 220 nm colloidal sphere) after water treatment with different magnifications. (a) ×1000; (b) ×5000; (c) ×20 000. The optical images of colorful FMs and corresponding reflective spectra with (d) 220, (e) 246, and (f) 280 nm colloidal spheres, respectively. The colorful pictures was cut and rebuilt from the original pictures as shown in Figure S3 in the Supporting Information.

Supporting Information shows the identical color of FM with different bending angles from 0 to 30°. The microstructure of FM was retained after bending 10 times with small angle (30°) as shown in the SEM image of Figure S5b in the Supporting Information, and also both the reflection peaks unshifted after bending 10 times in the reflection spectra (Figure S5c in the Supporting Information). However, the colorful FM would form cracks if bending with large angle because of the low adhesive force among the colloidal spheres after water treatment.

To further investigate the physical mechanism of the structural color induced by multiple reflection peaks, we assembled the colloidal nanospheres in capillary (Figure S6) to fabricate colorful colloidal crystal fibers (CCFs), as shown Figure 5a. The typical structure of CCFs is curved face-centered cubic (f.c.c.) (Figure 5b). The cross-sectional structure of the CCF, shown in the inset of Figure 5b, demonstrates that the curved (111) surface is parallel to the wall of capillary tube.[41] Green, orange, and red-colored CCFs were observed by the dark-field optical microscope. Corresponding reflective spectra were measured by angle-resolved microspectroscopy.[29] The CCFs' reflective spectras were calculated in accordance with the rigorous coupled wave analysis (RCWA) method based on the photonic band gap theory (detailed discussions in the Supporting Information, Figure S7).

Figure 5c shows a comparison of the FMs' and CCFs' reflective spectra, performed by redrawing the spectra as a function of the size parameter, $\pi r/\lambda$. The x-axis shows the dimensionless ratio of particle radius to light wavelength, eliminating particle size effect by normalizing the sizes. Two common features are observed around 0.65 and 1.06 for different FM samples. At 0.65, the spectra of FMs and CCFs show similar reflection peaks at the same size parameter, indicating those reflection peaks have the same physical origination. Because CCFs' optical properties have a highly periodic structure, the coincident peaks at 0.65 indicate the reflection peaks appearing at 533, 604,and 678 nm (Figure 4d−-f) are caused by the photonic band gap effect. The reflection around 1.06, as shown in Figure 6c, is attributed to Mie scattering,[42,43] as the reflection of CCFs does not exist around this region. The black-dashed curve in Figure 5c shows the scattering cross section of a single dielectric nanosphere (reflective index 1.6) embedded in air, calculated by Mie theory.[44] The general shape of the FMs' reflection spectra is similar to the reflection spectra explained by Mie theory. The lowest order Mie scattering peak appears around 0.9, and explains the high reflection of FMs around 1.06. The mismatch of the results between single particle Mie theory and FMs (composed of touching nanospheres) could be due to the multiple scattering processes of nanosphere clusters and coupling between the adjacent spheres.[45,46] As shown in Figure S8 in the Supporting Information, the electrospun FM packed with 280 nm spheres had a mixed color of purpl-red, which attributes to the dual visible reflections. However, the corresponding CCF and flat colloidal crystal film prepared by the same size spheres were purely red in color as a result of a

DOI: 10.1021/acsami.5b03289
ACS Appl. Mater. Interfaces 2015, 7, 14064−14071

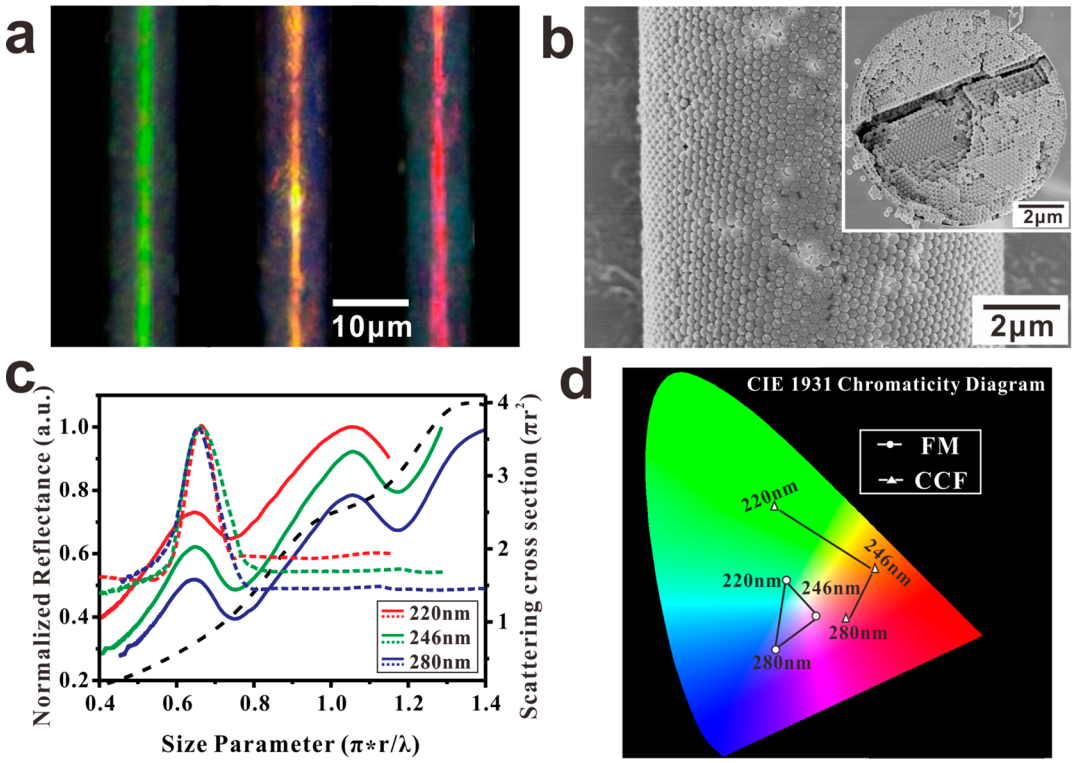

Figure 5. (a) Dark-field images of CCFs. (b) Typical SEM images of the surface and cross-section of CCF with 220 nm colloidal sphere. (c) CCFs and FMs reflective spectra as a function of the size parameter, $\pi r/\lambda$. FMs are marked in solid, whereas CCFs are marked with dashed lines; the black dashed curve is the scattering cross-section calculated by Mie theory. (d) CIE tristimulus values and chromaticity values of three colorful FMs and CCFs.

single peak in photonic reflection. It is evident that the structural colors of FM can be attributed to two mechanisms: photonic band gap effect relating to coherence scattering by partial ordered nanosphere arrangement, and resonant Mie scattering relating to incoherence scattering by numerous disordered nanosphere scatters.

In Figure 5d, the FMs' reflective peaks in the spectra are converted to Commission Internationale de L'Eclairage (CIE) tristimulus values (Table S1 in the Supporting Information); the corresponding chromaticity x and y values were plotted onto the CIE chromaticity diagram. The CIE values of CCFs structure are also plotted for comparison (Table S2 in the Supporting Information). The corresponding colors in CIE diagram match the observed color of the real fibrous samples. It is possible to almost cover the entire visible spectrum using the FMs from only three nanosphere sizes (220, 240, 280 nm); however, it is impossible to have such wide coverage through use of CCFs only with these three sizes. The wide coverage of these FMs is due to the mixture of colors from photonic band gap reflection and resonant Mie scattering.

Figure 6 shows FM color changes under different observation angles. Due to the cylindrical shape of the fiber and its electrospinning-induced disorder, the obtained FMs colors appear homogeneous and noniridescent. This characteristic is desirable because it is similar to the dye-based coloration presently used in industry. Figure 6a shows reflective spectra taken at different incident angles (0−40°) for a FM consisting of 220 nm nanospheres. The reflective peaks of the FM are independent of incident angles, since the spectral shifts of the peaks are unperceivable. The same angle independency was observed for FMs composed of 246 and 280 nm nanospheres (Figure S11 in the Supporting Information). In contrast to FMs, highly ordered 3D photonic crystal films (Figure S10 in the Supporting Information) prepared by self-assembly of the 220 nm nanospheres show strong angle dependence (the inset image of Figure 6a). Figure 6b shows dark-field colors of FM and flat photonic crystal film corresponding to the reflection spectra at different angles. The flat photonic crystal film colors shifted dramatically from green to blue as the incident angle changed from 0° to 40°; FM colors were unchanged. Furthermore, the optical pictures of FM packed with 246 nm nanospheres were taken with different observation angles from 0° to 40°, as shown in Figure S12 in the Supporting Information. It can be clearly observed that the colors are unchanged. The scattering property of the colorful FM was measured by fixing the incident angle at 0° (perpendicular to the surface of the sample, Figure S9 in the Supporting INformation) and collecting the scattered light around the reflective angle. Two reflective peaks of FM were unshifted (Figure 6c); the intensity of the reflective peaks gradually decreased when the collection angle deviated from reflective direction. For the flat photonic crystal films, scattering quickly vanished once it deviated from reflective direction (the inset image of Figure 6c). Figure 6d shows the dark-field colors from the scattering spectra. For the flat photonic crystal film, only green was exhibited in the direction of the reflection, whereas FM colors could be observed in directions deviating from the reflection. This indicates that FM exhibits isotropic color properties that are independent of incident and observing angles. Therefore, the coloration of the FM is similar to the color property in dyes, which are adapted from interpretations made by human vision.

DOI: 10.1021/acsami.5b03289
ACS Appl. Mater. Interfaces 2015, 7, 14064−14071

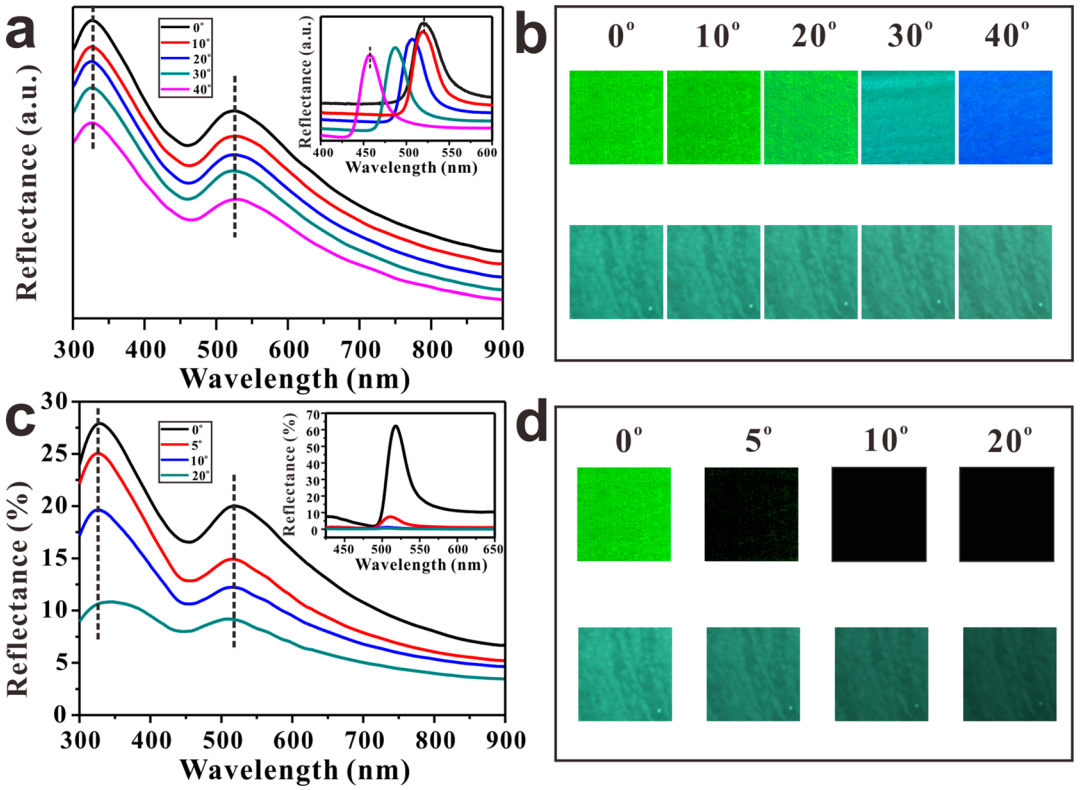

Figure 6. (a) Reflective spectra of FM and flat photonic crystal film (inset image) with different incident angles. (b) Dark-field optical images of the corresponding reflection spectra of flat photonic crystal film (upper panel) and FM (lower panel) with different incident angles. (c) Scattering spectra of FM and flat photonic crystal film (inset image) with different detection angles. (d) Dark-field optical images of the corresponding scattering spectra of flat photonic crystal film (upper panel) and FM (lower panel) with different detection angles. The diameter of the colloidal sphere is 220 nm.

CONCLUSIONS

In conclusion, dye-free electrospun FMs with noniridescent and tunable structural colors were fabricated via electrospinning. The obtained FMs are composed of individual colloidal fibers, several micrometers in diameter. The colloidal fibers are composed of monodisperse colloidal spheres possessing short-range order. The optical spectra indicate that the FMs' noniridescent and homogeneous colors originate from the reflectance of photonic band gap and Mie scattering. Full color display is achievable by changing the size of the colloidal spheres; it is possible to cover most of the entire visible spectrum using only three sizes of nanospheres. As this method is based on structural coloration rather than pigmentation, it presents an ecologically conscious alternative to the harmful dyeing practices used by the textile industry. This novel coloration method can be scaled up, making dye-free textile coloration possible. In the future, inorganic spheres with higher reflective indices (such as Fe_3O_4[47,48] and silicon[49,50]) can be used to fabricate colloidal fibers with polymer binders, via electrospinning. Because of the high refractive index contrast, the electrospun FM will show structural color without removing the binder, which can further increase the mechanical properties of such colored fibers.

ASSOCIATED CONTENT

Supporting Information

Experimental process of fabrication of colloidal crystal fibers and flat photonic crystal film; details on numerical calculation; thermogravimetric analysis of colloidal electrospun FM; size distribution of the obtained colloidal fibers; reflection spectrum of electrospun FM before water treatment; The original optical images of colorful FMs; bendability of colorful FM after water treatment; schematic illustration of the fabrication of CCFs; experimental and calculated reflective spectra of colloidal crystal fibers; schematic illustration of the experimental setups used for angle-independent; optical pictures of red-color FM with different observation angles from 0 to 40°; CIE tristimulus values and chromaticity values of FMs and CCFs. The Supporting Information is available free of charge on the ACS Publications website at DOI: 10.1021/acsami.5b03289.

AUTHOR INFORMATION

Corresponding Author

*E-mail: kqzhang@suda.edu.cn.

Notes

The authors declare no competing financial interest.

ACKNOWLEDGMENTS

We gratefully acknowledge the financial support from the National Science Foundation of China under Grant 51073113, 91027039, 51373110 and 11404064, the Natural Science Foundation of the Jiangsu Higher Education Institutions of China under Grant 10KJA540046 and Shanghai Pujiang Program (14PJ1401100). Lei Shi acknowledges the support from the Program for Professor of Special Appointment (Eastern Scholar) at Shanghai Institutions of Higher Learning. We also acknowledge support from the Priority Academic Program Development of Jiangsu Higher Education Institutions

DOI: 10.1021/acsami.5b03289
ACS Appl. Mater. Interfaces 2015, 7, 14064−14071

(PAPD), Qing Lan Project for Excellent Scientific and Technological Innovation Team of Jiangsu Province (2012) and Project for Jiangsu Scientific and Technological Innovation Team (2013).

REFERENCES

(1) Pauling, L. A Theory of the Color of Dyes. *Proc. Natl. Acad. Sci. U.S.A.* **1939**, *25*, 577−582.
(2) Martínez-Huitle, C. A.; Ferro, S. Electrochemical Oxidation of Organic Pollutants for the Wastewater Treatment: Direct and Indirect Processes. *Chem. Soc. Rev.* **2006**, *35*, 1324−1340.
(3) Mongkholrattanasit, R.; Kryštůfek, J.; Wiener, J. Dyeing and Fastness Properties of Natural Dyes Extracted from Eucalyptus Leaves Using Padding Techniques. *Fiber. Polym.* **2010**, *11*, 346−350.
(4) Montero, G. A.; Smith, C. B.; Hendrix, W. A.; Butcher, D. L. Supercritical Fluid Technology in Textile Processing: An Overview. *Ind. Eng. Chem. Res.* **2000**, *39*, 4806−4812.
(5) Kinoshita, S.; Yoshioka, S. Structural colors in nature: The Role of Regularity and Irregularity in the Structure. *ChemPhysChem* **2005**, *6*, 1442−1459.
(6) Kinoshita, S.; Yoshilka, S.; Miyazaki, J. Physics of Structural Colors. *Rep. Prog. Phys.* **2008**, *71*, 076401.
(7) Zhao, Y.; Xie, Z.; Gu, H.; Zhu, C.; Gu, Z. Bio-inspired Variable Structural Color Materials. *Chem. Soc. Rev.* **2012**, *41*, 3297−3317.
(8) Sun, J.; Bhushan, B.; Tong, J. Structural Coloration in Nature. *RSC Adv.* **2013**, *3*, 14862−14889.
(9) Zi, J.; Yu, X.; Li, Y.; Hu, X.; Xu, C.; Wang, X.; Liu, X.; Fu, R. Coloration Strategies in Peacock Feathers. *Proc. Natl. Acad. Sci. U.S.A.* **2003**, *100*, 12576−12578.
(10) Parker, A. R.; McPhedran, R. C.; McKenzie, D. R.; Botten, L. C.; Nicorovici, N. P. Photonic Engineering Aphrodite's Iridescence. *Nature* **2001**, *409*, 36−37.
(11) Kinoshita, S.; Yoshioka, S.; Fujii, Y.; Okamoto, N. Photophysics of Structural Color in the *Morpho* Butterflies. *Forma* **2002**, *17*, 103−121.
(12) Yoshioka, S.; Kinoshita, S. Effect of Macroscopic Structure in Iridescent Color of the Peacock Feathers. *Forma* **2002**, *17*, 169−181.
(13) Gao, X.; Yan, X.; Yao, X.; Xu, L.; Zhang, K.; Zhang, J.; Yang, B.; Jiang, L. The Dry-style Antifogging Properties of Mosquito Compound Eyes and Artificial Analogues Prepared by Soft Lithography. *Adv. Mater.* **2007**, *19*, 2213−2217.
(14) Whitney, H. M.; Kolle, M.; Andrew, P.; Chittka, L.; Steiner, U.; Glover, B. J. Floral Iridescence, Produced by Diffractive Optics, Acts as A Cue for Animal Pollinators. *Science* **2009**, *323*, 130−133.
(15) Parker, A. R.; Welch, V. L.; Driver, D.; Martini, N. Strcutural Colour: Opal Analogue Discovered in A Weevil. *Nature* **2003**, *426*, 786−787.
(16) Mie, G. Beiträge zur Optik Trüber Medien, Speziell Kolloidaler Metallösungen. *Ann. Phys.* **1908**, *25*, 377−445.
(17) Finger, E. Visible and UV Coloration in Birds: Mie Scattering as the Basis of Color in Many Bird Feathers. *Naturwissenschaften* **1995**, *82*, 570−573.
(18) Noh, H.; Liew, S. F.; Saranathan, V.; Mochrie, S. G. J.; Prum, R. O.; Dufresne, E. R.; Cao, H. How Noniridescent Colors Are Generated by Quasi-ordered Structures of Bird Feathers. *Adv. Mater.* **2010**, *22*, 2871−2880.
(19) Khudiyev, T.; Ozgur, E.; Yaman, M.; Bayindir, M. Structural Coloring in Large Scale Core-shell Nanowires. *Nano Lett.* **2011**, *11*, 4661−4665.
(20) Lee, I.; Kim, D.; Kal, J.; Baek, H.; Kwak, D.; Go, D.; Kim, E.; Kang, C.; Chung, J.; Jang, Y.; Ji, S.; Joo, J.; Kang, Y. Quasi-amorphous Colloidal Structures for Electrically Tunable Full-color Photonic Pixels with Angle-independency. *Adv. Mater.* **2010**, *22*, 4973−4977.
(21) Takeoka, Y.; Honda, M.; Seki, T.; Ishii, M.; Nakamura, H. Structural Colored Liquid Membrane without Angle Dependence. *ACS Appl. Mater. Interfaces* **2009**, *5*, 982−986.
(22) Prum, R. O.; Torres, R. H.; Williamson, S.; Dyck, J. Coherent Light Scattering by Blue Feather Barbs. *Nature* **1998**, *396*, 28−29.
(23) Yin, H.; Dong, B.; Liu, X.; Zhan, T.; Shi, L.; Zi, J.; Yablonovitch, E. Amorphous Diamond-structured Photonic Crystal in the Feather Barbs of the Scarlet Macaw. *Proc. Natl. Acad. Sci. U.S.A.* **2012**, *109*, 10798−10801.
(24) Dufresne, E. R.; Noh, H.; Saranathan, V.; Mochrie, S. G. J.; Cao, H.; Prum, R. O. Self-assembly of Amorphous Biophotonic Nanostructures by Phase Separation. *Soft Matter* **2009**, *5*, 1792−1795.
(25) Retsch, M.; Schmelzeisen, M.; Butt, H. J.; Thomas, E. L. Visible Mie Scattering in Non absorbing Hollow Sphere Powders. *Nano Lett.* **2011**, *11*, 1389−1394.
(26) Liu, Z.; Zhang, Q.; Wang, H.; Li, Y. Structural Colored Fiber Fabricated by A Facile Colloid Self-assembly Method in Micro-space. *Chem. Commun.* **2011**, *47*, 12801−12803.
(27) Liu, Z.; Zhang, Q.; Wang, H.; Li, Y. Magnetic Field Induced Formation of Visually Structural Colored Fiber in Micro-space. *J. Colloid Interface Sci.* **2013**, *406*, 18−23.
(28) Liu, Z.; Zhang, Q.; Wang, H.; Li, Y. Structurally Colored Carbon Fibers with Controlled Optical Properties Prepared by A Fast and Continuous Electrophoretic Deposition Method. *Nanoscale* **2013**, *5*, 6917−6922.
(29) Zhou, N.; Zhang, A.; Shi, L.; Zhang, K. Fabrication of Structurally-colored Fibers with Axial Core-shell Structure via Electrophoretic Deposition and Their Optical Properties. *ACS Macro Lett.* **2013**, *2*, 116−120.
(30) Finlayson, C. E.; Goddard, C.; Papachristodoulou, E.; Snoswell, D. R.E.; Kontogeorgos, A.; Spahn, P.; Hellmann, G. P.; Hess, O.; Baumberg, J. J. Ordering in Stretch-tunable Polymeric Opal Fibers. *Opt. Express* **2011**, *19*, 3144−3154.
(31) Kolle, M.; Lethbridge, A.; Kreysing, M.; Baumberg, J. J.; Aizenberg, J.; Vukusic, P. Bio-inspired Band-gap Tunable Elastic Optical Multilayer Fibers. *Adv. Mater.* **2013**, *25*, 2239−2245.
(32) Li, K.; Zhang, Q.; Wang, H.; Li, Y. Red, Green, Blue (RGB) Electrochromic Fibers for the New Smart Color Change Fabrics. *ACS Appl. Mater. Interfaces* **2014**, *6*, 13043−13050.
(33) Sun, X.; Zhang, J.; Lu, X.; Fang, X.; Peng, H. Mechanochromic Photonic-Crystal Fibers Based on Continuous Sheets of Aligned Carbon Nanotubes. *Angew. Chem., Int. Ed.* **2015**, *54*, 3630−3634.
(34) Tymczenko, M.; Marsal, L. F.; Trifonov, T.; Rodriguez, I.; Manzano, F. R.; Pallarès, J.; Rodríguez, Á.; Alcubilla, R.; Meseguer, F. Colloidal Crystal Wires. *Adv. Mater.* **2008**, *20*, 2315−2318.
(35) Wang, J. X.; Wen, Y. Q.; Ge, H. L.; Sun, Z. W.; Zheng, Y. M.; Song, Y. L.; Jiang, L. Simple Fabrication of Full Color Colloidal Crystal Films With Tough Mechanical Strength. *Macromol. Chem. Phys.* **2006**, *207*, 596−604.
(36) Yuan, W.; Zhang, K. Structural Evolution of Electrospun Composite Fibers from the Blend of Polyvinyl Alcohol and Polymer Nanoparticles. *Langmuir* **2012**, *28*, 15418−15424.
(37) Stoiljkovic, A.; Ishaque, M.; Justus, U.; Hamel, L.; Klimov, E.; Heckmann, W.; Eckhardt, B.; Wendorff, J. H.; Greiner, A. Preparation of Water-stable Submicron Fibers from Aqueous Latex Dispersion of Water-insoluble Polymers by Electrospinning. *Polymer* **2007**, *48*, 3974−3981.
(38) Li, D.; Xia, Y. Electrospinning of Nanofibers: Reinventing the Wheel? *Adv. Mater.* **2004**, *16*, 1151−1170.
(39) Greiner, A.; Wendorff, J. H. Electrospinning: A Fascinating Method for the Preparation of Ultrathin Fibers. *Angew. Chem., Int. Ed.* **2007**, *46*, 5670−5703.
(40) Spahn, P.; Finlayson, C. E.; Etah, W. M.; Snoswell, D. R.E.; Baumberg, J. J.; Hellmann, G. P. Modification of the Refractive-index Contrast in Polymer Opal Films. *J. Mater. Chem.* **2011**, *21*, 8893−8897.
(41) Moon, J. H.; Kim, S.; Yi, G.; Lee, Y.; Yang, S. Fabrication of Ordered Macroporous Cylinders by Colloidal Templating in Micro-capillaries. *Langmuir* **2004**, *20*, 2033−2035.
(42) Dong, B. Q.; Liu, X. H.; Zhan, T. R.; Jiang, L. P.; Yin, H. W.; Liu, F.; Zi, J. Structural Coloration and Photonic Pseudogap in Natural Random Close-packing Photonic Structures. *Opt. Express* **2010**, *18*, 14430−14438.

DOI: 10.1021/acsami.5b03289
ACS Appl. Mater. Interfaces 2015, 7, 14064−14071

(43) Saranathan, V.; Forster, J. D.; Noh, H.; Liew, S.; Mochrie, S. G. J.; Cao, H.; Dufresne, E. R.; Prum, R. O. Structure and Optical Function of Amorphous Photonic Nanostructures from Avian Feather Barbs: A Comparative Small Angle X-ray Scattering (SAXS) Analysis of 230 Bird Species. *J. R. Soc. Interfaces* **2012**, *9*, 2563−2580.
(44) Doicu, A.; Wriedt, T.; Eremin, Y. A. In *Light Scattering by Systems of Particles*; Springer: Berlin, 2006; Chapter 2, pp 99−102.
(45) Sapienza, R.; García, P. D.; Bertolotti, J.; Martín, M. D.; Blanco, Á.; Viña, L.; López, C.; Wiersma, D. S. Observation of Resonant Behavior in the Energy Velocity of Diffused Light. *Phys. Rev. Lett.* **2007**, *99*, 233902.
(46) García, P. D.; Sapienza, R.; López, C. Photonic Glasses: A Step Beyond White Paint. *Adv. Mater.* **2010**, *22*, 12−19.
(47) Ge, J.; Yin, Y. Magnetically Tunable Colloidal Photonic Structures in Alkanol Solutions. *Adv. Mater.* **2008**, *20*, 3485−3491.
(48) Ge, J.; Hu, Y.; Biasini, M.; Beyermann, W. P.; Yin, Y. Superparamagnetic Magnetite Colloidal Nanocrystal Clusters. *Angew. Chem., Int. Ed.* **2007**, *46*, 4342−4345.
(49) Shi, L.; Tuzer, T. U.; Fenollosa, R.; Meseguer, F. A New Dielectric Metamaterial Building Block with a Strong Magnetic Response in the Sub-1.5-Micrometer Region: Silicon Colloid Nanocavities. *Adv. Mater.* **2012**, *24*, 5934−5938.
(50) Shi, L.; Harris, J. T.; Fenollosa, R.; Rodriguez, I.; Lu, X.; Korgel, B. A.; Meseguer, F. Monodisperse Silicon Nanocavities and Photonic Crystals with Magnetic Response in the Optical Region. *Nat. Commun.* **2013**, *4*, 1904.

DOI: 10.1021/acsami.5b03289
ACS Appl. Mater. Interfaces 2015, 7, 14064−14071